In vivo measurement of retinal physiology with high-speed ultrahigh-resolution optical coherence tomography

V. J. Srinivasan, M. Wojtkowski, and J. G. Fujimoto

Department of Electrical Engineering and Computer Science and Research Laboratory of Electronics, Massachusetts Institute of Technology, Cambridge, Massachusetts 02139

J. S. Duker

New England Eye Center, Tufts-New England Medical Center, Tufts University School of Medicine, Boston, Massachusetts 02111

Received March 8, 2006; revised May 8, 2006; accepted May 17, 2006; posted May 18, 2006 (Doc. ID 67783); published July 10, 2006

Noninvasive *in vivo* functional optical imaging of the intact retina is demonstrated by using high-speed, ultrahigh-resolution optical coherence tomography (OCT). Imaging was performed with 2.8 μm resolution at a rate of 24,000 axial scans per second. A white-light stimulus was applied to the dark-adapted rat retina, and the average reflectivities from different intraretinal layers were monitored as a function of time. A 10%–15% increase in the average amplitude reflectance of the photoreceptor outer segments was observed in response to the stimulus. The spatial distribution of the change in the OCT signal is consistent with an increase in backscatter from the photoreceptor outer segments. To our knowledge, this is the first *in vivo* demonstration of OCT functional imaging in the intact retina.

OCIS codes: 110.4500, 170.3660, 170.3880.

Optical measurement of neural physiology has become an active area of research. Small changes in optical properties caused by membrane depolarization and cell swelling have been measured in the brain cortex.[1,2] Recent studies using fundus reflectometry and flash stimuli have demonstrated retinal reflectance changes that may be indicative of retinal function.[3–5] Optical coherence tomography (OCT) provides fine depth resolution and high sensitivity to light scattered from tissue. OCT imaging of neural activity was demonstrated in the sea slug ganglion[6] and the cat visual cortex.[7] Recent work using time domain OCT demonstrated measurement of retinal functional changes in response to a flash stimulus.[8,9] These studies showed changes in OCT signals in the photoreceptor inner and outer segments and ganglion cell layer[9] and were performed by using excised *ex vivo* retinal preparations. The observed changes were attributed to photoreceptor disc membrane hyperpolarization in response to a strong stimulus. *In vivo* functional OCT measurements in the intact eye are challenging because of ocular motion and speckle noise. OCT with "spectral/Fourier domain" detection[10] can perform high-speed data acquisition,[11,12] which permits new scanning and signal averaging protocols that can achieve the low noise and high sensitivities required for *in vivo* functional OCT.

A high-speed, ultrahigh-resolution OCT (UHR-OCT) system was used for functional imaging in the rat retina. The spectrometer has been described previously[13] and was adapted for a broadband superluminescent diode light source (two-diode Broadlighter with $\lambda_0 = 890$ nm, bandwidth 145 nm, Superlum Diodes, Ltd.). A microscope delivery system was developed for imaging the small animal eye. The system used two microscope objectives (10×, NA = 0.28, and 5×, NA = 0.14, Mitutoyo Long Working Distance Objectives) and two galvanometers with scanning mirrors (Cambridge Technology, Inc.). Postobjective scanning was used to eliminate aberrations associated with scanning through an objective lens. A 10 μm FWHM transverse spot with a confocal parameter of 120 μm provided adequate depth of field for retinal imaging. The working distance was 15 mm. After digitally shaping the spectrum[14] to reduce sidelobes in the point spread function, the axial resolution in the eye was 2.8 μm. Dispersion imbalance between the sample and reference interferometer arms was numerically compensated. The incident power at the cornea was 620 μW, and the measured system sensitivity was 95 dB. The imaging speed was 24,000 axial scans per second.

Long–Evans rats were anesthetized with sodium pentobarbital (Nembutal) (40–50 mg/kg intraperitoneal). After anesthesia, eyes were dilated with topical tropicanimide (Mydriacyl, 1%). The animal was placed in a comfortable holder with its head in a mount to minimize eye motion. Hydroxypropyl methylcellulose (Goniosol, 2.5%) was used to maintain corneal hydration, and a thin glass coverslip was gently placed on the cornea to remove curvature and permit focusing of the OCT beam on the retina. All animal procedures were performed at MIT facilities with protocol approval by the MIT Committee on Animal Care.

For functional OCT experiments, animals were first dark-adapted for 12 h, then dark-adapted for 30 min between subsequent trials. A transient white-light stimulus (1.3 s and 1400 cd/m^2) was delivered during the functional recording while OCT imaging was performed on a selected region of the retina to

0146-9592/06/152308-3/$15.00

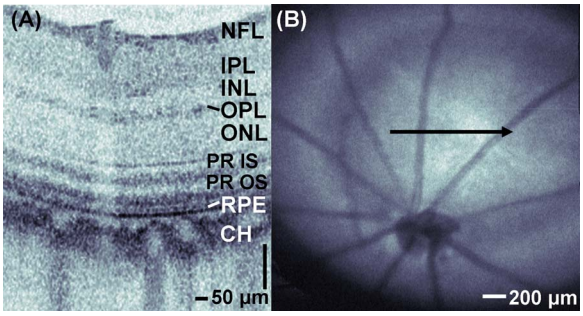

Fig. 1. (Color online) (A) OCT cross-sectional scan of the rat retina, with (B) an OCT fundus image and arrow showing the scan location. NFL, nerve fiber layer; IPL, inner plexiform layer; INL, inner nuclear layer; OPL, outer plexiform layer; ONL, outer nuclear layer; PR IS, photoreceptor inner segments; PR OS, photoreceptor outer segments; RPE, retinal pigment epithelium; CH, choroid.

measure reflectance changes. The OCT light source bandwidth spanned 817–962 nm, well outside the sensitivity range of the rat retina. The white-light stimulus duration and intensity were chosen to prevent photoreceptor bleaching. In some trials, preadaptation with 1.3 s of 1400 cd/m^2 white light was performed 2 min before the functional OCT recording. Stimulus intensities were verified by electroretinogram recordings and are well below levels required for photoreceptor bleaching.

A baseline recording without any stimulus was performed prior to the functional recording. During each recording, a 160 μm $\times$ 160 μm transverse (*en face*) region of the retina was measured repeatedly with a raster scan pattern. This scanning protocol repeatedly acquires 3D volumes of $64 \times 64 \times 1024$ pixels. Each volume is acquired in 162 ms, corresponding to a rate of 6.2 volumes/s. Transverse eye motion artifacts were corrected by cross correlation and cropping of consecutive data sets. To monitor the reflectance from the photoreceptor outer segments, the photoreceptor inner segment/outer segment (IS/OS) junction was used as a reference surface, and all axial scans were shifted to flatten the IS/OS boundary. To register the functional measurement location, an OCT fundus image, obtained by axial summation of 3D OCT data, was created. An example of a cross-sectional image and corresponding OCT fundus image are shown in Figs. 1(A) and 1(B).

The results of the functional imaging experiments are shown in Figs. 2–4. Each data point shown in Fig. 2 is obtained by averaging the photoreceptor outer segment reflectance from one volume acquired in 162 ms. The physiologic noise from the baseline recording had a standard deviation $<1\%$ (squares in Fig. 2). The functional recording showed that a white-light stimulus induced an $\sim 12\%$ increase in the average amplitude reflectance from the outer segments (circles in Fig. 2). A white-light stimulus applied after preadaptation induced a significantly smaller response of $\sim 2\%$ (triangles in Fig. 2), with a time course similar to the dark-adapted response. Both the dark-adapted and preadapted reflectance changes in response to the stimulus are statistically significant ($p < 0.01$). After 30 min of dark adaptation subsequent to a stimulus trial, a response similar in time course, amplitude, and location to the original dark-adapted response was observed.

The observed reflectance change was largest in the photoreceptor outer segments and was localized to the region between the photoreceptor IS/OS junction and the retinal pigment epithelium, as shown in Fig. 3(A). The data from one volume is unwrapped, flattened to the IS/OS junction, and displayed as an image in Fig. 3(B), with major intraretinal layers labeled for reference. To emphasize the similarities between the preadapted and dark-adapted functional response topographies near the outer segments, the two curves are overlaid in Fig. 4(A) and plotted on different amplitude scales. Because the reflectance change after preadaptation is near the physiologic

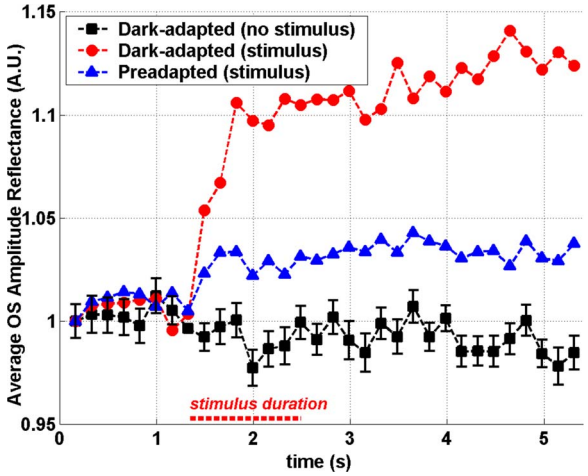

Fig. 2. (Color online) Dark-adapted and preadapted functional response time courses compared with the baseline response. Each data point corresponds to the amplitude reflectance from the photoreceptor outer segments averaged over a single volume. Each error bar (± standard deviation) represents the standard deviation of the amplitude reflectance difference referenced to the stimulus onset ($t = 1.3$ s).

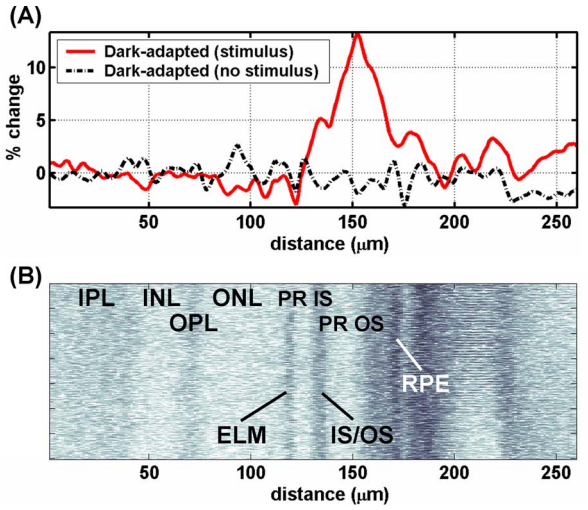

Fig. 3. (Color online) (A) Plot of the percent change in photoreceptor outer segment amplitude reflectance for $t > 2.6$ s compared with $t < 1.3$ s. (B) The data from one volume are unwrapped, flattened to the IS/OS boundary, and displayed as a log scale image for comparison with (A).

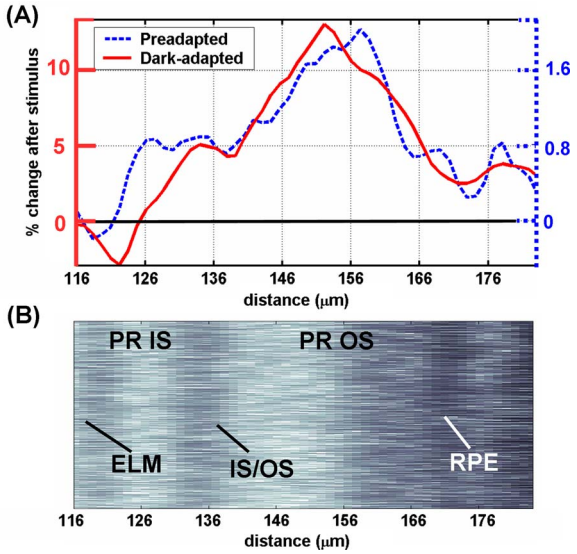

Fig. 4. (Color online) (A) Plot of the percent change in photoreceptor outer segment amplitude reflectance for $t > 2.6$ s compared with $t < 1.3$ s for the dark-adapted and preadapted trials. (B) The OCT data from one volume are unwrapped, flattened to the IS/OS boundary, and displayed as a log scale image for comparison with (A).

noise level, the data from three trials were averaged to obtain the preadapted curve in Fig. 4(A). The topography of the reflectance change is similar for both cases (dark-adapted and preadapted), although the amplitude is reduced after preadaptation. Figure 4(B) shows an unwrapped volume, for comparison with Fig. 4(A).

Previous studies using fundus imaging techniques have shown photoreceptor reflectance changes that are not attributable to visual pigment absorption.[3,15] When compared with other fundus imaging techniques, OCT provides axial resolutions approaching 2–3 μm and has high sensitivity to weakly backscattering structures. These two features permit the detection of highly localized optical changes in the retina. While the observed amplitude reflectance change of 12% (25% intensity reflectance change) was large, the maximum reflectance change is observed over an axial depth range of approximately 10 μm. The absolute magnitude of this change represents a small fraction of the total light backscattered from the fundus.

The observed reflectance changes are consistent with a scattering change near the photoreceptor outer segments and may be related to previous findings in *ex vivo* retinal preparations.[8,9] The optical signal may be due to structural changes in the outer segment disks, membrane hyperpolarization and cell swelling, or changes in the interphotoreceptor matrix constituents. Histochemical studies on rats have shown that major components of the interphotoreceptor matrix undergo a shift after the transition between light and dark.[16] The physiological origin of the observed reflectance changes is the subject of current investigations.

In conclusion, functional imaging is demonstrated in the intact rat retina *in vivo* using high-speed, UHR-OCT. A backscattering change in the photoreceptor outer segments is observed in response to a white-light stimulus. This response is reduced after preadaptation and restored after dark-adaptation. These results constitute an advance over previous *ex vivo* studies because noninvasive measurements can be performed in an intact eye. These studies may eventually aid in detecting alterations of retinal function during the early stages of disease.

We acknowledge contributions of Sven Bursell, Alan Clermont, and Jonathan Liu. Maciej Wojtkowski is currently at Nicholas Copernicus University in Torun, Poland. J. Fujimoto receives royalties from intellectual property licensed by MIT to Carl Zeiss Meditec. This research was sponsored in part by the National Science Foundation BES-0522845, the National Institutes of Health R01-EY011289-20 and EA75289-09, and the Air Force Office of Scientific Research FA9550-040-1-0046 and FA9550-040-1-0011. V. Srinivasan's e-mail address is vjsriniv@mit.edu.

References

1. A. Grinvald, R. D. Frostig, E. Lieke, and R. Hildesheim, Physiol. Rev. **68**, 1285 (1988).
2. A. Villringer and B. Chance, Trends Neurosci. **20**, 435 (1997).
3. K. Tsunoda, Y. Oguchi, G. Hanazono, and M. Tanifuji, Invest. Ophthalmol. Visual Sci. **45**, 3820 (2004).
4. D. A. Nelson, S. Krupsky, A. Pollack, E. Aloni, M. Belkin, I. Vanzetta, M. Rosner, and A. Grinvald, Invest. Ophthalmol. Visual Sci. **36**, 57 (2005).
5. M. D. Abramoff, Y. H. Kwon, D. Ts'o, P. Soliz, B. Zimmerman, J. Pokorny, and R. Kardon, Invest. Ophthalmol. Visual Sci. **47**, 715 (2006).
6. M. Lazebnik, D. L. Marks, K. Potgieter, R. Gillette, and S. A. Boppart, Opt. Lett. **28**, 1218 (2003).
7. R. U. Maheswari, H. Takaoka, H. Kadono, R. Homma, and M. Tanifuji, J. Neurosci. Methods **124**, 83 (2003).
8. K. Bizheva, R. Pflug, B. Hermann, B. Povazay, H. Sattmann, P. Qiu, E. Anger, H. Reitsamer, S. Popov, J. R. Taylor, A. Unterhuber, P. Ahnelt, and W. Drexler, Proc. Natl. Acad. Sci. U.S.A. **103**, 5066 (2006).
9. X. C. Yao, A. Yamauchi, B. Perry, and J. S. George, Appl. Opt. **44**, 2019 (2005).
10. A. F. Fercher, C. K. Hitzenberger, G. Kamp, and S. Y. Elzaiat, Opt. Commun. **117**, 43 (1995).
11. M. Wojtkowski, T. Bajraszewski, P. Targowski, and A. Kowalczyk, Opt. Lett. **28**, 1745 (2003).
12. N. A. Nassif, B. Cense, B. H. Park, M. C. Pierce, S. H. Yun, B. E. Bouma, G. J. Tearney, T. C. Chen, and J. F. de Boer, Opt. Express **12**, 367 (2004).
13. M. Wojtkowski, V. J. Srinivasan, T. H. Ko, J. G. Fujimoto, A. Kowalevicz, and J. S. Duker, Opt. Express **12**, 2404 (2004).
14. R. Tripathi, N. Nassif, J. S. Nelson, B. H. Park, and J. F. de Boer, Opt. Lett. **27**, 406 (2002).
15. P. J. DeLint, T. T. Berendschot, J. van de Kraats, and D. van Norren, Invest. Ophthalmol. Visual Sci. **41**, 282 (2000).
16. F. Uehara, M. T. Matthes, D. Yasumura, and M. M. Lavail, Science **248**, 1633 (1990).